Dinh *et al. Geoscience Letters* (2025) 12:38
https://doi.org/10.1186/s40562-025-00410-9

Geoscience Letters

RESEARCH LETTER

Open Access

Geomorphic constraints on differential surface uplift across the Dien Bien Phu Fault, northwestern Vietnam, and its implications on crustal dynamics in the southeastern Tibetan Plateau

Thi-Hue Dinh[1*], Chih-Tung Chen[1*] and Yu-Chang Chan[2]

Abstract

At the southeastern frontier of the propagating India–Asia collision, the Dien Bien Phu Fault in northwestern Vietnam provides a good opportunity to study the growth and crustal dynamics of the Tibetan Plateau; however, full activity of the fault remains poorly constrained, particularly the vertical component. This study offers, for the first time, new constraints on surface uplift pattern across the fault based on quantitative tectonic geomorphology analyses (normalized steepness index, and erosion rate from fluvial shear stress) combined with mapping of river terraces. The results from geomorphic indices exhibit a conspicuous concurrence between regions of high normalized steepness index and of high erosional rate values that are spatially concentrated on the W/NW side of the Dien Bien Phu Fault. The results from the preliminary terrace mapping are also consistent with the spatial trends of the geomorphic indices, indicated by the larger elevation separations between terrace levels on the W/NW side of the fault. Since non-tectonic factors including climate and lithology do not systematically vary across the Dien Bien Phu Fault, such spatial consistence indicates a significant higher uplift on the W/NW side of the fault. Considering that the observed uplift is not concentrated near the fault trace but distributed in the whole fault block, we postulate crustal thickening in the W/NW side of the Dien Bien Phu Fault through arrival of ductile mid-to-lower crust flow propagating from the Tibetan Plateau.

Keywords Normalized steepness index, Fluvial erosional rates, River terraces, Differential surface uplift, The Dien Bien Phu Fault, India–Asia collision

Introduction

The tectonic evolution of the Tibetan Plateau and surrounding regions has attracted much attention over the past few decades to gain insights to continental geodynamics (e.g., Burchfiel and Royden 1985; England and Houseman 1986; Kirby and Ouimet 2011; Molnar et al. 1993; Shen et al. 2005; Tapponnier et al. 1982, 1986; Wang and Barbot 2023). The development of the plateau is generally regarded as a consequence of the ongoing collision between the Indian and Asian continents, which commenced around the middle Paleocene (Hu et al. 2016;

*Correspondence:
Thi-Hue Dinh
dinhhue91@g.ncu.edu.tw
Chih-Tung Chen
chihtung@cc.ncu.edu.tw
[1] Department of Earth Sciences, National Central University, Taoyuan City, Taiwan
[2] Institute of Earth Sciences, Academia Sinica, Taipei City, Taiwan

Molnar and Tapponnier 1975; Wu et al. 2023). After the collision, the Asian continent was broken into large crustal fragments which extruded laterally along major strike-slip faults as envisaged in the rigid block extrusion model (e.g., Akciz et al. 2008; Tapponnier et al. 1982, 1986), taking the continental lithosphere as rigid micro-plates with strain concentrated along block boundaries delineated by large strike-slip faults. The continuing underthrusting of the Indian continent also caused significant crustal thickening to around 70–90 km in southern to central Tibet (e.g., Allégre et al. 1984; Rai et al. 2006; Wittlinger et al. 2004). With such anomalous crustal thickness, roughly doubled from a normal continental crust, rheology is expected to alter with occurrence of a weak ductile mid to lower crust (e.g., Burchfiel 2004; Royden et al. 1997, 2008) which might form outward flow due to the continuing indenting Indian continent. This channelized ductile flow has been proposed to be responsible for the observed E–W extension, causing normal faulting activities in central Tibet and left-lateral slips along N–S trending strike-slip faults in eastern margin of the plateau (e.g., Liu 2003; Royden et al. 2008; Wang et al. 2010a, b). In this perspective, this thickened continental lithosphere can be viewed as a ductile medium of distributed strain, and has been propagating eastward and southeastward via the Kunlun Fault and the Haiyuan Fault to the Longmenshan–Minshan margin, and southeastward transport via the Xianshuihe–Xiaojiang Fault and the Dien Bien Phu Fault to Indochina regions, respectively (e.g., Burchfiel 2004; Pan and Shen 2017; Wang and Barbot 2023). While characteristics of active tectonic deformation of the Xianshuihe–Xiaojiang fault system have been studied in detail (e.g., Chen et al. 2020; Liu et al., 2021; Yu et al. 2022), those for the Dien Bien Phu Fault, particularly surface uplift patterns, remain poorly documented and are key to constrain plateau propagation processes at the southeastern frontier of the India–Asia collision (Bui et al. 2017; Lai et al. 2012; Zuchiewicz et al. 2004). Hence, assessing active differential vertical movement across the Dien Bien Phu Fault is expected to provide better understanding on crustal dynamics as consequence of the continent–continent collision, and can be achieved through river geomorphological analyses.

As the southeastern boundary of the plateau associated with crustal materials transporting toward southeast of Tibet, the Dien Bien Phu Fault in northwestern Vietnam provides an exceptional opportunity to study far-field effects of the India–Asia collision and tectonic processes responsible for propagation of the Tibetan Plateau. The Dien Bien Phu Fault is the most seismically active fault in the Indochina region, with two large recorded earthquakes of estimated Mw 6.0–7.0 happened in 1935 and 1983 (Chevalier et al. 2022). Tectonic geomorphology studies (e.g., Lai et al. 2012; Zuchiewicz et al. 2004) indicated that the Dien Bien Phu Fault is predominantly a left-lateral strike-slip fault. However, the vertical component of fault offsets remained generally unrecognized while significant in understanding the crustal geodynamics. Here we attempt to bridge this gap by investigating presence of active differential surface uplift across the Dien Bien Phu Fault through river geomorphology: (1) normalized steepness index of stream profiles is extracted for a preliminary survey of tectonic signals across the fault; (2) erosional rate from fluvial shear stress of the drainage systems is calculated and integrated with the normalized steepness index values to better reveal the pattern of differential surface uplift; (3) river terraces are identified and mapped using DEM topography cross-checked with satellite imagery and published geological maps. The results indicate higher surface uplift in the W/NW side of the Dien Bien Phu Fault, and such vertical offset might imply differential crustal thickening across the fault as a major tectonic boundary.

Geological setting

Northern Vietnam, located to the southeast of the eastern Himalayan syntaxis, is tectonically linked to the Tibetan Plateau as evidenced in activities along the Red River Fault (Fig. 1a, e.g., Lee and Lawver 1995; Li et al. 2020; Schoenbohm et al. 2006; Tapponnier et al. 1982, 1990a, b). This region experienced two main tectonic events: the first Indosinian event began with the closure of the Paleo-Tethys and followed by the collision of the Indochina and the South China in the Triassic time (e.g., Faure et al. 2014; Lepvrier et al. 2004), and the second Himalayan event as the collision between the Indian and Asian continents in the Cenozoic time (e.g., Lee and Lawver 1995; Searle 2006; Searle et al. 2010; Tapponnier et al. 1990a, b). The assembly of lithologies and the thrust contacts among them were largely achieved during the Indosinian episode (Faure et al. 2014), while the southeastward propagation of Himalayan collision has led to reactivation of these structures into strike-slip faults (e.g., Leloup et al. 2001; Schärer et al. 1990; Tapponnier et al. 1990a, b) or strike-slip faults with normal slip component (Jolivet et al. 2001; Viola and Anczkiewicz 2008; Yeh et al. 2008). Among these structures, the Dien Bien Phu Fault is the most active one in geodetic and seismic perspectives (e.g.,Cong and Feigl 1999; Lu et al. 2016), and may connect northward with the sinistral Xiaojiang and Xianshuihe faults (Fig. 1b).

The Dien Bien Phu Fault, located in the west of northern Vietnam, is approximately 150 km long, with rupture zone around 6–10 km wide, and north-to-northeast trending. Along the fault trace, the Dien Bien Phu Fault cuts through sedimentary and metamorphic rocks of

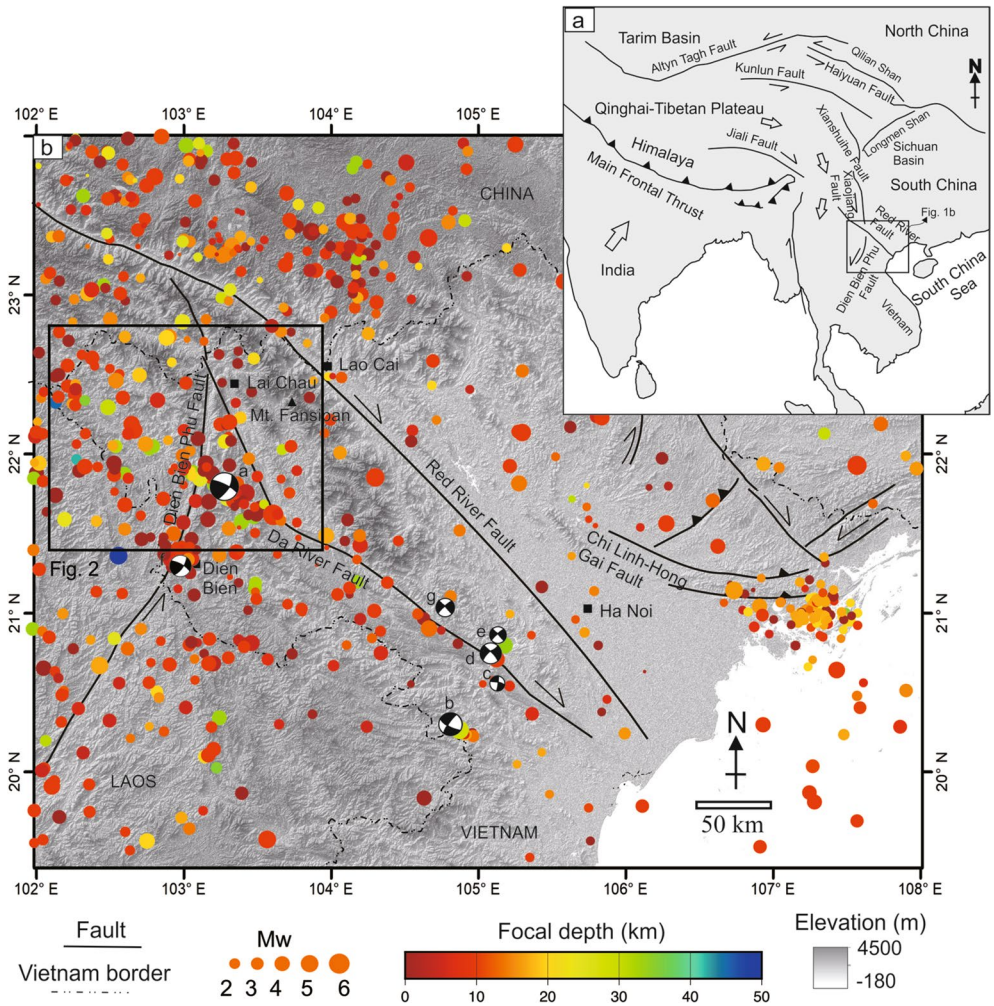

Fig. 1 **a** Tectonic sketch showing active faults and recent movements of the Tibetan Plateau and its surrounding regions (Modified from Zhang et al. 2004). Black arrow indicates movement of the faults. Big white arrows present relative movement of blocks with respect to stable Eurasia. **b** Topographic map showing location of the main faults and seismicity in northern Vietnam. Seismic events (1980–2020) were downloaded from website http://www.isc.ac.uk/. Focal mechanisms of the earthquakes occurred on: a—1983, Mw 6.7; b—1985, Mw 5.7; c—1989, Mw 3.7; d—1989, Mw 4.9; e—1989, Mw 4.0; f—2001, Mw 5.1; g—2020, Mw 5.0 (Compiled from Chevalier et al. (2022) and Cong & Feigl (1999)

Paleozoic to Mesozoic times, as well as intrusives of Paleozoic and Triassic times named the Dien Bien Phu complex (Fig. 2a, e.g., Lin et al. 2009; Zuchiewicz et al. 2004). Among them, the Dien Bien Phu complex has attracted much attention as evidence of a right lateral displacement along the fault (e.g., Bui et al. 2017; Lin et al. 2009; Roger et al. 2014), for which the timing is constrained to be Early Jurassic and considered as a response to the far-field effects of successive collisions between the Indochina, Simao, and Sibumasu continental blocks following the Indosinian Orogeny (Lin et al. 2009). Recent activity of the Dien Bien Phu Fault is left-lateral with extension that commenced in the Pliocene (Lai et al. 2012). The activity of the Dien Bien Phu Fault is suggested to be related to the Xianshuihe–Xiaojiang fault system, the most seismically active fault in the southeastern border of Tibetan Plateau, as they have consistent spatial alignment and shear sense (Burchfiel 2004; Lai et al. 2012; Zhang et al. 2004). The occurrence of left-slip and extension along the Xianshuihe–Xiaojiang and Dien Bien Phu faults has been proposed to result from lower crustal flow and clockwise rotation around the eastern Himalayan syntaxis and the Dien Bien Phu Fault is, therefore, considered the southeastern frontier of the current plateau propagation (e.g., Burchfiel 2004; Royden et al. 2008; Zhang et al. 2004). Hence, understanding characteristics of active tectonic deformation of the Dien Bien Phu Fault is critical in gaining insights to the crustal/lithospheric

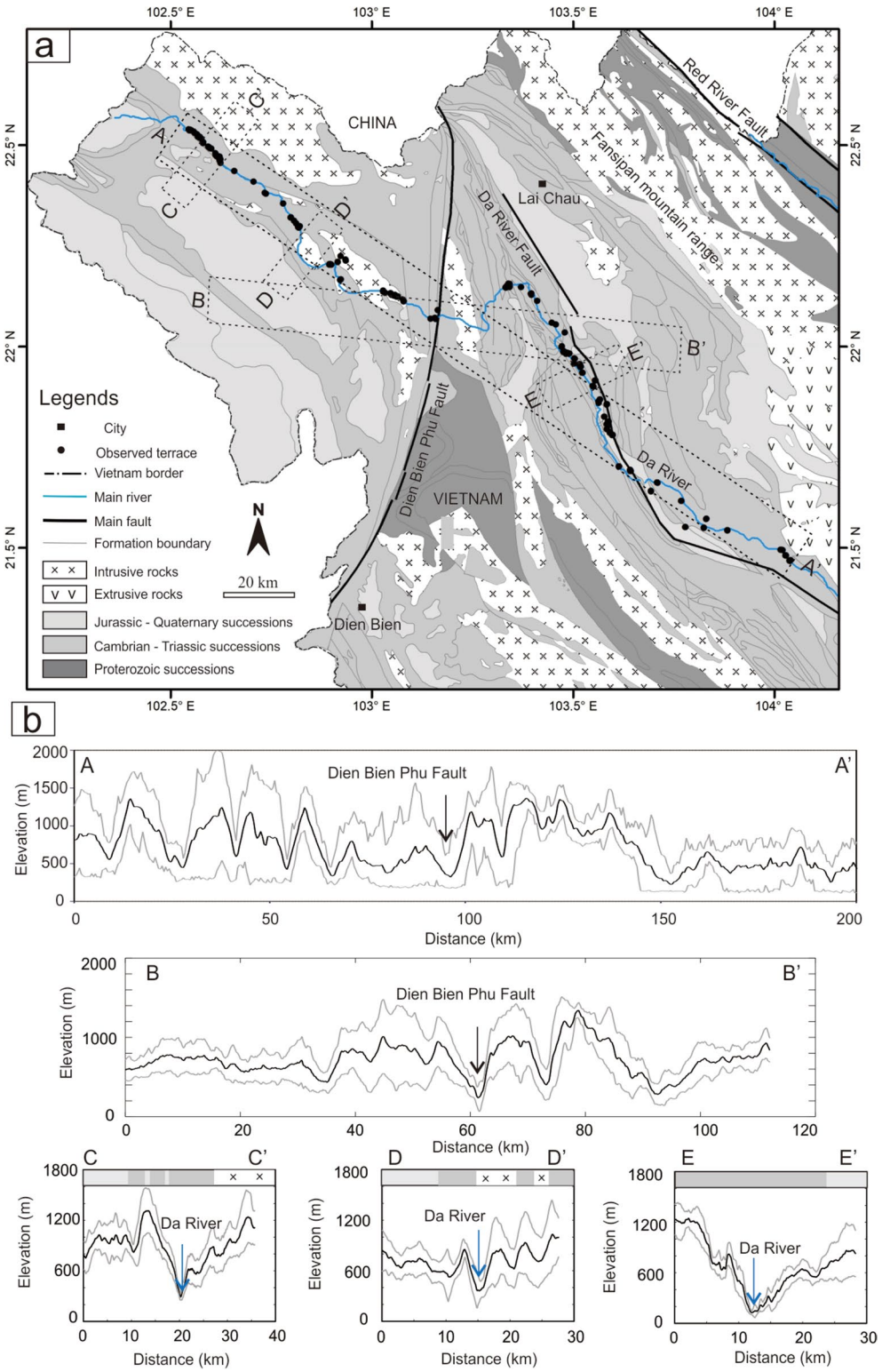

Fig. 2 **a** Simplified geological map of the study area with locations of Da River and the observed terraces. **b** Topographic swath profiles AA', BB', CC', DD', and EE'. Locations of their swath profiles are shown in **a**. The lithology units are shown above the swath profiles—CC', DD', and EE' with the colors corresponding to the same color in the geological map as shown in **a**

dynamics driving active growth and development of the plateau.

Methodology

This study analyzes geomorphic indices including normalized steepness index and erosional rate from fluvial shear stress, as well as surveys of river terrace geomorphology based on the ALOS PALSAR 12.5-m, ASTER 30-m DEMs data (downloaded from the websites https://asf.alaska.edu and https://search.earthdata.nasa.gov/search, respectively) in conjunction with high-resolution Google Earth optical imagery (from https://earth.google.com), to constrain spatial variations in relative surface uplift across the active Dien Bien Phu Fault.

Normalized steepness index

The normalized steepness index of rivers is analyzed to investigate the spatial distribution of differential surface uplift pattern (e.g., Kirby et al. 2007; Kirby and Ouimet 2011; Whipple and Gasparini 2014). The fundamental idea of this method is that the change in river channel elevation is the result of interaction between erosion and uplift (Wobus et al. 2006), and can be expressed as the following equation:

$$\mathrm{d}z/\mathrm{d}t = U(x,t) - KA^{\mathrm{m}}S^{\mathrm{n}}$$

where $\mathrm{d}z/\mathrm{d}t$ is the change in elevation through the time; U (x, t) is the rock uplift rate relative to a fix base level; K is the erosion coefficient; A is upstream drainage area; S is gradient; and m, n are positive constants. Under a steady state ($\mathrm{d}z/\mathrm{d}t=0$), the above equation can be rewritten as

$$S = [U(x,t)/K]^{1/\mathrm{n}}A^{-\mathrm{m}/\mathrm{n}} = k_{\mathrm{s}}A^{\Theta}$$

where Θ indicates the concavity index; and the steepness index (k_{s}) is expressed by a function of rock uplift rate: $k_{\mathrm{s}}=[U(x,t)/K]^{1/n}$; and therefore, it is considered as useful ones to derive quantitative estimates of relatively uplift rate. As the concavity index varies among rivers, to compare steepness of different rivers, the river steepness should be converted to normalized steepness index (k_{sn}) by adopting a reference concavity (Θ_{ref}) often set to 0.45 (e.g., Kirby and Whipple 2012; Wobus et al. 2006). Normalized steepness index values (k_{sn}) can thus be derived utilizing MATLAB functions on the DEMs data and mapped to infer variations in relative tectonic uplift across the study area assuming similar K and precipitation.

Erosional rate from fluvial shear stress

Because of postulated feedback between surface erosion and tectonic uplift in equilibrium topography, analysis of erosional rate from fluvial shear stress was also carried out for an independent tectonic uplift evaluation. Due to a strong correlation with river incision, fluvial shear stress was widely invoked to estimate erosional rate (e.g., Godard et al. 2010; Lavé and Avouac 2001; Ye et al. 2022). The fluvial shear stress of river channel (τ) can be expressed by the following equation:

$$\tau = \rho g \frac{(QN)^{3/5}S^{7/10}}{W^{3/5}}$$

where ρ is water density; g is gravitational acceleration; S is channel slope; W is channel width; N is channel roughness coefficient correlated with grain size of river bed sediments; and Q is discharge that can be expressed as a power-law function of drainage area (A) as follows:

$$Q = \mathrm{k}PA^{0.85}$$

where P is the annual precipitation; and k is an empirical constant. The fluvial shear stress of river (τ) can be converted to erosional rate (i) via a non-dimensional parameter, Shields stress (τ*). Shields stress (τ*) and erosional rate (i) can be calculated as follows:

$$\tau^* = \frac{\tau}{(\rho_s - \rho)gD_{50}}$$

$$i = K(\tau * - \tau *_{\mathrm{c}})$$

where ρ_{s} and ρ is density of bedrocks and water, respectively; D_{50} is grain diameter of materials; K is erodibility; τ^*_{c} is the critical Shields stress values and the approximate value of the critical Shields stress is about 0.03. Once the required parameters including S, W, N, Q, P, A, D_{50}, ρ_{s}, and K are determined, the values of fluvial shear stress and erosional rate can be calculated. In this study, river channel slope (S) and drainage area (A) are derived using ALOS PALSAR 12.5-m, ASTER 30-m DEM data, processed with ArcGIS software. Channel width (W) is extracted from Google Earth images. The average annual precipitation over the catchment was estimated using monthly climate data (1970–2000) provided by WorldClim 2.1 (Fick and Hijmans 2017), processed with ArcGIS software for spatial analysis. The empirical constant k was derived using a 21-year data set of discharge (1989–2010), with an average value of around 55.5×10^9 m^3/year, obtained from the Hoa Binh station, the largest gauging station on the Da River (Vinh et al. 2014). As the largest gauging station located downstream on the Da River, Hoa Binh station may serve as a representative site for discharge estimation. To estimate discharge (Q) at ungauged locations, we apply the relationship $Q=\mathrm{kPA}^{0.85}$ (e.g., Lavé and Avouac 2001; Ye et al. 2022), where P is average precipitation and A is drainage area. Using the

known discharge value at the Hoa Binh gauging station with its corresponding P and A values, we calculated the empirical constant k. This value was then used to estimate discharge (Q) at other survey points within the Da River system. Due to the rugged topography and limited accessibility of the Da River, field measurements of sediment grain size (D_{50}) were not feasible. However, field observations and previous report (e.g., Nguyen 2006) indicate that sediments in the upstream section are dominated by gravels and cobbles. Accordingly, the corresponding sediment grain size (D_{50}) of 0.5 cm and channel roughness coefficient (N) of 0.1 are adopted (Whipple 2004). The erodibility (K) values of ~ 1.6 and ~ 3.2 mm/yr, along with density (ρ_s) of 2700 kg/m^3 and 2500 kg/m^3 for granitoids and sedimentary bedrocks, respectively (Ye et al. 2022) are incorporated. Detailed parameter values used for calculating the erosion rate along the Da River can be found in Supplementary Appendix S1. Negative values of erosion rate were obtained at certain locations where the computed Shields stress (τ^*) was lower than the critical threshold (τc^*). These values are considered non-physical meaningful and reflect the limitation of the linear relationship $i = K(\tau^* - \tau c^*)$. In this study, such values were set to zero to ensure consistency and comparability across the data set. Given the scale of the study, this simplified adjustment is not expected to significantly impact the overall results.

River terrace mapping

River terraces are step-like landforms resulting from river system responses to regional uplift and climatic influences, and are thus considered key geomorphic features recording climate changes and tectonic activities (Burbank and Anderson 2011). Systematic investigation of river terraces was lacking in the concerned northwestern Vietnam, which is pivotal in constraining differential surface uplift across the region of rather uniform humid subtropical climate. In this research, river terrace mapping in northwestern Vietnam is attempted by interpreting DEM data and Google Earth images with aids from published literatures and geological maps. We first identify areas of low relief and quasi-planer surface along river channels on Google Earth images as examples shown in Fig. 3, and verify our mapping by crosschecks with detailed maps along (segments of) the Red River Fault (Trinh et al. 2012) and the Dien Bien Phu Fault (Lai et al. 2012). Elevations of these preliminary-mapped terrace surfaces are extracted by integrating Google Earth with the ALOS PALSAR 12.5-m and ASTER 30-m DEMs data. Once the elevation values are obtained, terrace locations are plotted along longitudinal river profiles and the primary sequence of terrace system can be established.

Results

Normalized steepness index value

To illuminate differential surface uplift surrounding the Dien Bien Phu Fault, normalized steepness index (k_{sn}) has been calculated for the entire river network with a drainage area greater than 10^7 m^2. The resultant k_{sn} values for the whole study area are exhibited in Fig. 4. Distribution of k_{sn} values on opposing sides of the Dien Bien Phu Fault are quite distinct: high k_{sn} values of over 250 m$^{0.9}$, marked by orange and red colors, are more frequent on the W/NW side of the fault; the E/SE side of the fault, with a few exceptions, is characterized by relatively lower k_{sn} values marked in blue to green with the values of less than 200 m$^{0.9}$ (Fig. 4). Similar trend can be found along the main channel of the Da River, a major river draining orthogonal across the fault, with conspicuously higher k_{sn} value (22 m$^{0.9}$) in the upstream segment W/NW of the fault than in the downstream part to the E/SE (around 10 m$^{0.9}$) as shown in Fig. 5b. Overall, the value of k_{sn} on W/NW side of the fault is relatively higher than that on the S/SE side, suggesting the presence of a relatively high surface uplift rate on this side of the Dien Bien Phu Fault.

Erosional rate derived from fluvial shear stress

The erosional rate values determined from fluvial shear stress are calculated along the Da River across both sides of the Dien Bien Phu Fault (Figs. 4 and 5a). The derived erosional rate ranges from 0 to 2.0 mm/yr on the W/NW side of the fault, compared with 0 to 0.6 mm/yr on the E/SE side. Higher values of erosional rate, shown by dark blue color (Fig. 4), are more frequent on the W/NW side of the fault; similar pattern is exhibited in the histogram (Fig. 5a) showing values scattered with ~ 30% more than 0.2 mm/yr to the W/NW of the fault, while over 90% less than 0.2 mm/yr to the E/SE. Overall, the result from erosional rate values is in good agreement with k_{sn} values with relatively higher values on the W/NW side than the E/SE side of the Dien Bien Phu Fault.

River terrace distribution and characteristics of terrace sequences

The distribution of the observed river terraces along the Da River based on Google Earth imagery interpretation and ALOS PALSAR 12.5-m, and ASTER 30-m DEM data cross-check is presented in Fig. 3 and the detail information of terrace data is listed in Supplementary Appendices S2 and S3. The elevation of the observed terraces is also plotted along the longitudinal profile of Da River (Fig. 5c), and up to 3 terrace levels can be recognized. Vertical separations among terrace levels and riverbed are rather constant among each other E/SE of the fault, with the first terrace level close to the river bed at approximately 100 m above sea level

Fig. 3 **a** Topographic map showing distribution of the observed terraces along the Da River. **b–g** Satellite imagery (Downloaded from Google Earth, 2023) shows examples of the observed terraces along the Da River

and the second and the third terrace levels at around 120–130 m and 140–150 m, respectively; in contrast, this regular pattern disappears W/NW of the fault with increasing vertical separations from the fault trace toward the divide, likely implying different tectonic characteristics with respect to the E/SE side of the Dien Bien Phu Fault under rather uniform regional climate.

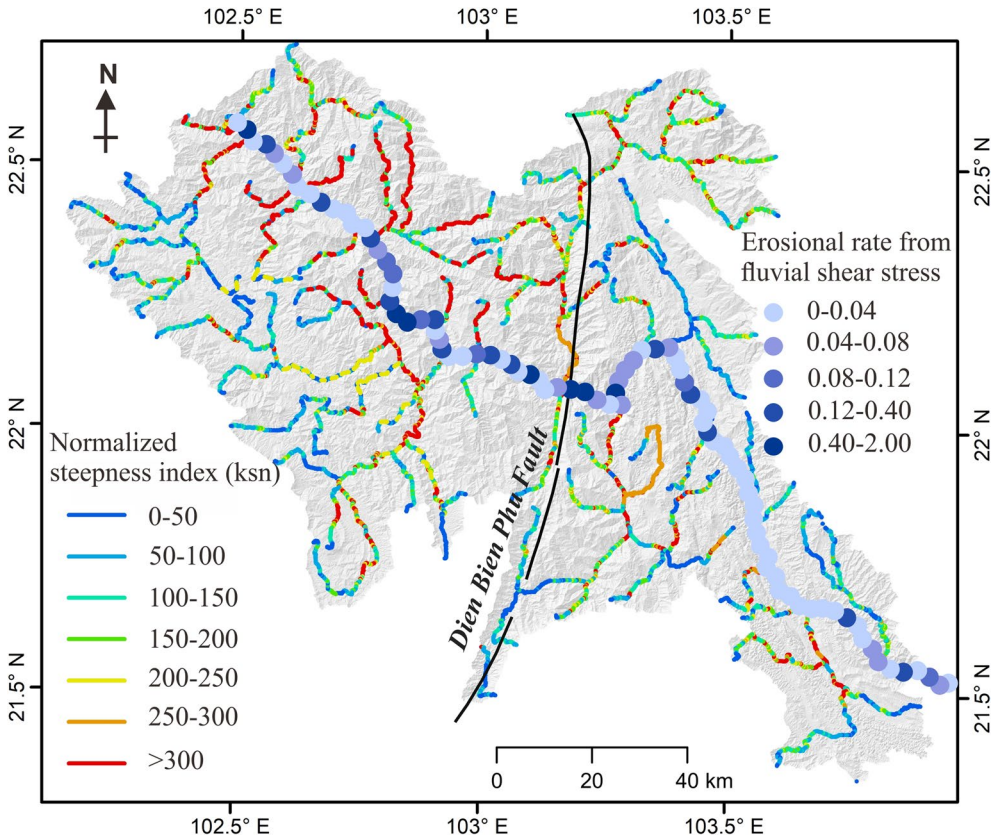

Fig. 4 Normalized steepness index values across the Dien Bien Phu Fault and erosional rate values along the Da River

Discussion

Differential surface uplift patterns across the Dien Bien Phu Fault

Key observations that emerge from our geomorphic analyses are: (1) high k_{sn} values are mostly distributed on the W/NW side of the Dien Bien Phu Fault (Figs. 4 and 5b); (2) the erosional rate extracted from fluvial shear stress is higher on the W/NW side of the fault compared to the other side (Figs. 4 and 5a); and (3) the elevated vertical separations between different terrace levels also observed on the W/NW side of the fault (Fig. 5c). Besides tectonic factors, effects from lithology and climate have to be discussed for these observed data variations.

Different lithology and climate (particularly precipitation variations) settings can alter the shape of river profile and thus may affect values of k_{sn} in the study area. Data compiled from the official geological map (Fig. 2) and the published literatures (e.g.,Lai et al. 2012; Roger et al. 2014) exhibit that (meta-) sedimentary rocks are the most common rock type in the study area, indicating that the observed variations of k_{sn} values are not primarily contributed by lithology effects. Regional precipitation data (Do et al. 2020) demonstrates that no substantial changes exist in rainfall amount across northwestern Vietnam with an average annual precipitation value of around 1500–1800 mm/yr. Therefore, non-tectonic factors including lithology and climate alone are unable to account for the observed k_{sn} value changes in our study area, particularly across the Dien Bien Phu Fault. In other words, tectonics is likely to be the main factor for differential k_{sn} values in the study area and thus, the concentrated distribution of high k_{sn} values on the W/NW

(See figure on next page.)

Fig. 5 **a** Erosional rate values (black dots) and their frequency distributions (gray lines and rectangles) in the NW and SE of the Dien Bien Phu Fault. The lithology units are shown below with the colors corresponding to the same color in the geological map as shown in Fig. 2a. **b** Longitudinal river profile of the Da River (black line) and the values of the normalized steepness index (k_{sn}) in the different sides of the Dien Bien Phu Fault. The triangles show the beginning and the end of the regression. Upper right rectangle shows log–log plots of gradient and drainage area data, which were used to calculate the k_{sn} values of the regressed segments. **c** Longitudinal river profile (black line) and the analyzed terrace correlations along the Da River. Black circle, red triangle, and green square—with bar show different levels of terraces

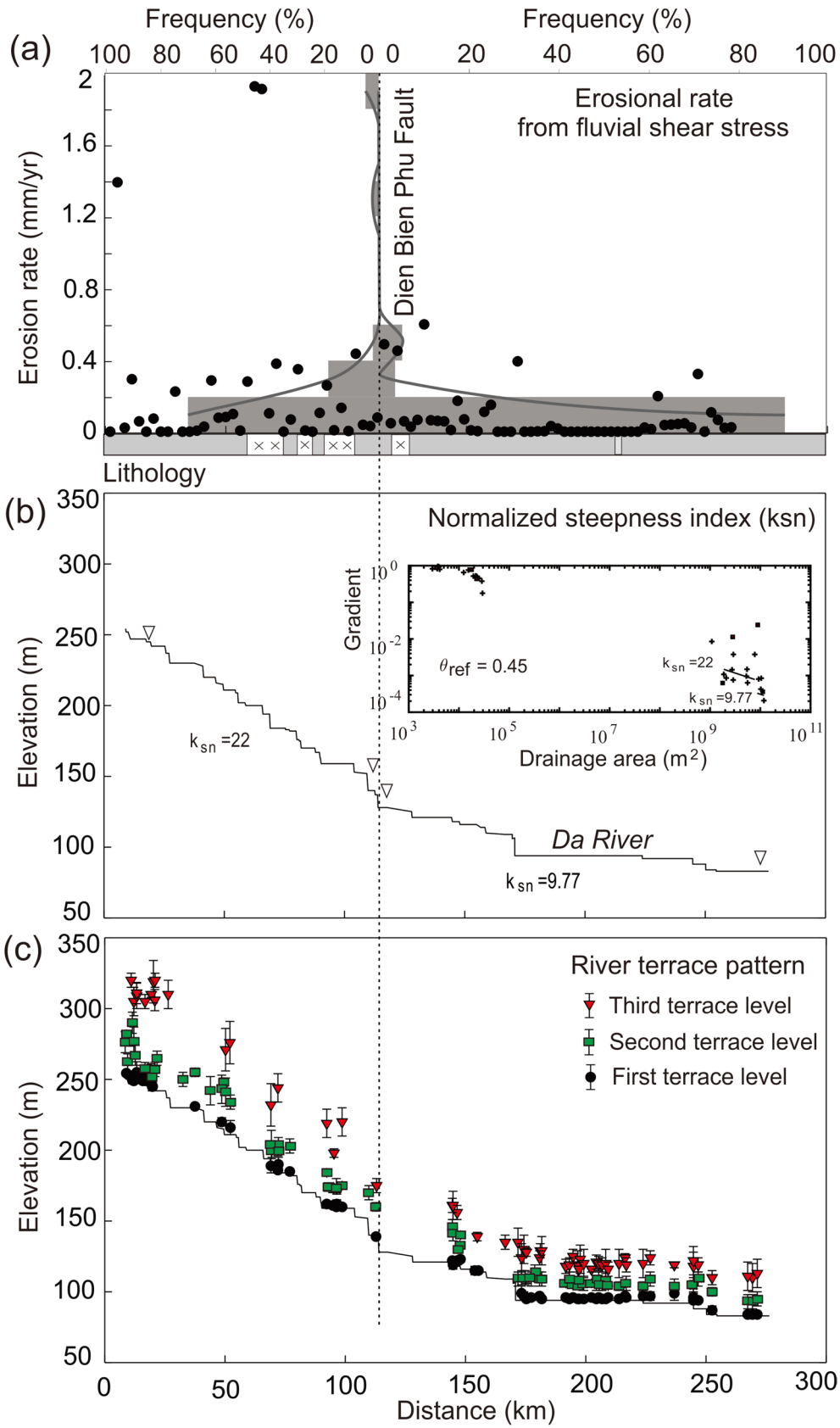

Fig. 5 (See legend on previous page.)

side of the Dien Bien Phu Fault implies a relatively higher uplift rate compared to the other side.

The values of erosional rate are similarly affected by climate, bedrock lithology and tectonics. Climate forcing plays a vital role on controlling extent of surface erosion by runoff intensity. Considering the average temperature and precipitation data (Schmidt-Thomé et al. 2014), the climate condition is rather constant over the entire study area, suggesting that climate forcing seems not capable in producing the observed erosional rate differences. Variation in lithology may influence erosional rate values, as river flowing across different rock types with different levels of erodibility. Thus, to evaluate the potential influence of lithology on erosional rates, we imposed lithological units on the resulting erosion rates values (Fig. 5a). In general, high values of erosional rates would be expected in areas dominated by sedimentary/metasedimentary rocks, which are typically less resistant to erosion than igneous or high-grade metamorphic rocks due to their fine-grained composition and weaker consolidation. However, our results show no significant correlation between erosional rate and lithology as high erosion values observed in both igneous and sedimentary/metasedimentary units. In addition, the highest erosional rates of approximately 2 mm/yr, that typically be expected in areas dominated by sedimentary/metasedimentary rocks, are instead occur in regions of igneous rocks as shown in Fig. 5a. Therefore, we suggest that lithology has minimum influence on the spatial variation of erosional rates in our study area. Similarly, to examine the potential control of lithology on topography, we also overlaid lithological units onto the swath profiles CC', DD', and EE' (Fig. 2b) to observe how elevation varies across different rock types. The results indicate that elevation patterns appear largely independent of lithology. For example, in swath profile CC', the elevation of sedimentary/metasedimentary unit (SW side of Da River) is even higher than that of igneous rocks (NE side of Da River). In swath profile DD', although lithology varies along the profile, the elevation remains nearly constant. Conversely, in swath profile EE', where a significant difference in elevation is observed, the lithology remains largely the same across the profile. These examples further support the interpretation that lithology is not primary factor effected spatial variation of erosional rates in this study. Since forcings of climate and lithology are insufficient to explain the observed spatial variation of erosional rate across the Dien Bien Phu Fault, differential tectonic uplift enhanced on the W/NW side is considered the major factor. This agrees with documented positive correlation between tectonic uplift and erosion in many orogenic and tectonically active regions, including the eastern margin of Tibetan Plateau (e.g., Cook et al. 2018) and the northern Andes (e.g., Ott et al. 2023), based on the rationale of equilibrium topography.

Formation of river terrace is controlled not only by neotectonics, but also by non-tectonic factors, such as sea-level fluctuations and climate changes. However, the study area located far from the sea, both in terms of geographic distance and elevation perspectives, eustatic sea-level changes are unlikely to have a significant impact. In addition, since the region has a relatively uniform subtropical monsoon climate, climatic factors are not deemed capable in triggering the observed expanding vertical separations among the three terrace levels W/NW of the Dien Bien Phu Fault. The diverging and elevated terrace levels are thus primarily the result of surface uplift, likely driven by ongoing crustal movements. This pattern is similar to other river terrace systems in tectonically active regions, such as the Himalayas and Taiwan, where dramatic vertical separation of terraces occurs due to intense tectonic uplift (e.g., Dutta et al. 2012; Joshi et al. 2022; Liew et al., 1990).

In summary, the most striking observation regarding geomorphic analyses across the Dien Bien Phu Fault is the concurrence among the region of high normalized steepness index, high erosional rate, and high vertical separations of river terraces spatially distributed on the W/NW side. Given that non-tectonic factors, including climate, lithology, and sea-level effects having negligible influences, the spatial association of the high values of normalized steepness index, erosional rate, and vertical separations between terrace levels are best attributed to a relatively higher tectonic uplift rate on this side of the fault as compared to the E/SE side.

Tectonic implications for crustal dynamics

As previously discussed, the spatial correspondence between regions of high normalized steepness indices, high erosion rates and wide terrace level separations suggests relatively higher uplift rate on the W/NW side of the Dien Bien Phu Fault as compared to its E/SE side, while the relative uplift detected is not concentrated in the near-fault area as commonly seen in elastic fault dislocations (e.g., Geist and Yoshioka 2004; Qiu et al. 2024). Such spatially distributed uplift in the entire western fault block, even with likely westward/northwestward increase as seen in the amplifying terrace elevation separations upstream (Fig. 5c), suggests ongoing crustal thickening on this side of the fault.

In addition, seismic data from northern Vietnam (Ha et al. 2024) indicate the occurrence of a low velocity zone of both P and S waves beneath the W/NW side of the Dien Bien Phu Fault. The lowest S-wave velocity anomaly occurs at depths of around 20 km to over 30 km and terminates almost under the fault trace, with little to no extension into the E/SE side (Fig. 6). This low velocity zone implies the presence of weak ductile materials in

mid-to-lower-crust beneath the W/NW side of the Dien Bien Phu Fault. The spatial coincidence between this deep weak crust and surface uplift inferred from geomorphic analyses led us to speculate that the underlying weak crustal zone, part of the deep ductile mass arriving from the Tibetan–Himalayan collision, may have facilitated crustal thickening on the W/NW side of the Dien Bien Phu Fault.

A similar geodynamic scenario has also been documented along the Xianshuihe–Xiaojiang Fault, where several geological and geophysical studies indicate that the western region of this fault has experienced crustal thickening and a low-seismic velocity in the mid-to-lower crust, which have been further interpreted as indicative of ductile mid-to-lower crustal flow propagating from the Tibetan Plateau (e.g., Bai et al. 2010; Wang et al. 2010a, b; Yang et al. 2020). Notably, the Dien Bien Phu Fault is widely regarded as the southeastern continuation of the Xianshuihe–Xiaojiang Fault system, based on both spatial alignment and kinematic characteristics (e.g., Burchfiel 2004; Lai et al. 2012; Shen et al. 2005). Given this tectonic linkage, it is plausible that the ductile channel flow along the Xianshuihe–Xiaojiang Fault could extend into the Dien Bien Phu region. This ductile channel flow could be resulted from thermal weakening of rheology through anomalous thickening of continental crust (e.g., Clark et al. 2004; Royden et al. 2008) and/or asthenosphere upwelling during lithospheric delamination (Chung et al., 1998). Under the bulldoze of Indian continent, the weak ductile mid-to-lower crust of adjacent Tibetan Plateau would be driven eastward and southeastward as channelized flow accompanied by tugged movements of the overlying brittle crust fragments (Royden et al. 2008; Tan et al. 2017). In this context, the Dien Bien Phu Fault may represent a part of the current front of the propagating mid-to-lower crust ductile flow, which thickens the crust west of the fault and facilitates enhanced differential uplift (Fig. 6). The hypothesized channelized ductile flow and the resultant surface uplift may still be advancing southeastward with the Dien Bien Phu Fault merely serving as a temporary propagation front, or may be buttressed along the fault if it constitutes a significant

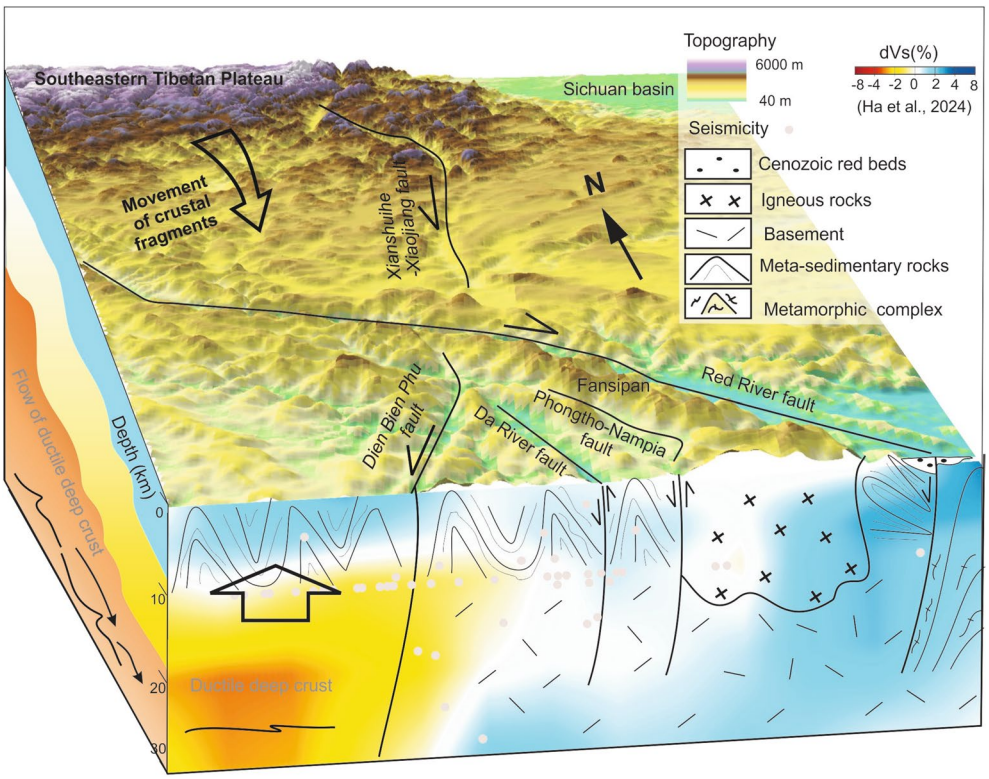

Fig. 6 Plausible tectonic model illustrating surface uplift and recent movements along the Dien Bien Phu Fault. S-wave velocity structure beneath northern Vietnam is modified from Ha et al. (2024). As the India continually bulldozing the Asia continent, the weak ductile mid-to-lower crust could be induced as a consequence of an over-thickened continental crust beneath the Tibetan Plateau (Royden et al. 2008). This weak ductile layer is expected to propagate eastward and southeastward as channelized flow, accompanied by the related movement of the overlying brittle crustal fragments. The arrival of such a channelized flow together with movements of the upper crustal fragment from the southeastern Tibetan Plateau could have accounted for differentially thickening the crust with relatively high uplift on the W/NW side and left-lateral displacement along the Dien Bien Phu Fault. Please refers to section "Tectonic implications for crustal dynamics" for more details

upright crustal discontinuity as reactivation of a major Jurassic dextral fault (Lin et al. 2009). The presence of differential surface uplift across the the Dien Bien Phu Fault, and the possible crustal thickening due to existence of mid-to-lower crust ductile flow W/NW of the fault, have significant implications for seismic hazard assessment and crustal rheology of northern Vietnam and also offers a valuable contribution to understanding the deformation processes in SE Asia. We acknowledge that this tectonic interpretation remains a speculative hypothesis and is proposed here as a plausible model rather than a definitive conclusion. More geophysical studies, such as seismic tomography, crustal receiver function analysis, or magnetotelluric imaging, are needed to verify the rheological constituents and presence of the ductile channel flow beneath our study area, and further elucidate regional tectonic dynamics.

Conclusions

We present a new geomorphic data to constrain vertical displacement of the Dien Bien Phu Fault, northwestern Vietnam. The results from this study show a significant association among regions of high normalized steepness indices, high erosional rates and wide terrace separations spatially distributed on the W/NW side of the fault. Given that non-tectonic effects appeared to play minimal roles, tectonics seems to be the dominant factor driving the observed differential geomorphic pattern. Thus, the spatial variation of geomorphic pattern is possibly associated with differential surface uplift across the Dien Bien Phu Fault with a significant high uplift rate on the W/NW side as compared to the E/SE side. Integrating our results with existing data, we postulate that active movements of the Dien Bien Phu Fault are associated with deep tectonic processes of the Tibetan Plateau orogenic system. As the India continually bulldozing the Asian continent, induce the ductile mid-to-lower crust could be produced in the thickened lithosphere beneath the Tibetan Plateau, which would extrude radially outside the plateau and propagate toward southeastward throughout the N-to-NE-trending active faults. The arrival of a such channelized mid-to-lower crust ductile flow could thus differentially thicken the crust and uplift the W/NW side of the Dien Bien Phu Fault.

Supplementary Information

The online version contains supplementary material available at https://doi.org/10.1186/s40562-025-00410-9.

Supplementary material 1.

Acknowledgements

This research was financially supported by the Ministry of Science and Technology (MOST) and the National Science and Technology Council (NSTC) of Taiwan under the project numbers: MOST 110-2116-M-008-008, MOST 111-2116-M-008-002, NSTC 112-2116-M-008-001, and NSTC 113-2628-M-008-003-MY3 to C.-T. Chen, as well as MOST 110-2811-M-008-540, MOST 111-2811-M-008-056, and NSTC 112-2811-M-008-036 to T.-H. Dinh. We sincerely thank Editor Prof. Kenji Satake and the two anonymous reviewers for their constructive and helpful comments, that have strengthened the interpretation model and improved the clarity and overall quality of the manuscript.

Author contributions

T.-H. Dinh: paper writing, analyzing geomorphic indices and mapping river terraces, and tectonic interpretation C.-T. Chen: project planning, tectonic interpretation, and writing—review, and editing Y.-C. Chan: tectonic interpretation and writing—review and editing.

Data availability

No data sets were generated or analyzed during the current study.

Declarations

Competing interests

The authors declare no competing interests.

Received: 10 April 2025 Accepted: 5 August 2025
Published online: 20 August 2025

References

Akciz S, Burchfiel BC, Crowley JL, Jiyun Y, Liangzhong C (2008) Geometry, kinematics, and regional significance of the Chong Shan shear zone, Eastern Himalayan Syntaxis, Yunnan, China. Geosphere 4:292–314. https://doi.org/10.1130/GES00111.1

Allégre CJ, Courtillot V, Tapponnier P, Hirn A, Mattauer M, Coulon C, Jaeger JJ, Achache J, Schärer U, Marcoux J, Burg JP, Girardeau J, Armijo R, Gariépy C, Göpel C, Tindong L, Xuchang X, Chenfa C, Guangqin L, Baoyu L, Jiwen T, Naiwen W, Guoming C, Tonglin H, Xibin W, Wanming D, Huaibin S, Yougong C, Ji Z, Hongrong Q, Peisheng B, Songchan W, Bixiang W, Yaoxiu Z, Xu R (1984) Structure and evolution of the Himalaya-Tibet orogenic belt. Nature 307:17–22. https://doi.org/10.1038/307017a0

Bai D, Unsworth MJ, Meju MA, Ma X, Teng J, Kong X, Sun Y, Sun J, Wang L, Jiang C, Zhao C, Xiao P, Liu M (2010) Crustal deformation of the eastern Tibetan Plateau revealed by magnetotelluric imaging. Nat Geosci 3:358–362. https://doi.org/10.1038/ngeo830

Bui HB, Ngo XT, Khuong TH, Golonka J, Nguyen TD, Song Y, Itaya T, Yagi K (2017) Episodes of brittle deformation within the Dien Bien Phu Fault zone, Vietnam: evidence from K-Ar age dating of authigenic illite. Tectonophysics 695:53–63. https://doi.org/10.1016/j.tecto.2016.12.006

Burbank DW, Anderson RS (2011) Tectonic geomorphology. Wiley, Hoboken

Burchfiel BC (2004) New technology; new geological challenges. GSA Today. https://doi.org/10.1130/1052-5173(2004)014%3c0004:NTNGC%3e2.0.CO:2

Burchfiel BC, Royden LH (1985) North-south extension within the convergent Himalayan region. Geology 13:679. https://doi.org/10.1130/0091-7613(1985)13%3c679:NEWTCH%3e2.0.CO;2

Chen Y, Zhang G, Lu R, Luo T, Li Y, Yu W (2020) Formation and evolution of Xianshuihe Fault Belt in the eastern margin of the Tibetan Plateau: constraints from structural deformation and geochronology. Geol J 55:7953–76. https://doi.org/10.1002/gj.3908

Chevalier ML, Tapponnier P, Trinh PT, Briais A, Haibing LI, Rui XU (2022) Large-scale inversion of Plio-Quaternary slip along the boundary faults between the South China, Sunda, and Shan blocks. Acta Geol Sin. https://doi.org/10.19762/j.cnki.dizhixuebao.2022166.Marie

Clark MK, Schoenbohm LM, Royden LH, Whipple KX, Burchfiel BC, Zhang X, Tang W, Wang E, Chen L (2004) Surface uplift, tectonics, and erosion of eastern Tibet from large-scale drainage patterns. Tectonics 23:1–21. https://doi.org/10.1029/2002TC001402

Cong DC, Feigl KL (1999) Geodetic measurement of horizontal strain across the Red River fault near Thac Ba, Vietnam, 1963–1994. J Geod 73:298–310. https://doi.org/10.1007/s001900050247
Cook KL, Hovius N, Wittmann H, Heimsath AM, Lee YH (2018) Causes of rapid uplift and exceptional topography of Gongga Shan on the eastern margin of theTibetan Plateau. Earth Planet Sci Lett 481:328–337. https://doi.org/10.1016/j.epsl.2017.10.043
Do QV, Do HX, Do NC, Ngo AL (2020a) Changes in precipitation extremes across Vietnam and its relationships with teleconnection patterns of the northern hemisphere. Water. https://doi.org/10.3390/W12061646
Dutta S, Suresh N, Kumar R (2012) Climatically controlled late Quaternary terrace staircase development in the fold- and -thrust belt of the Sub Himalaya. Palaeogeogr Palaeoclimatol Palaeoecol 356–357:16–26. https://doi.org/10.1016/j.palaeo.2011.05.006
England P, Houseman G (1986) Finite strain calculations of continental deformation: 2. comparison with the India-Asia Collision Zone. J Geophys Res Solid Earth 91:3664–3676. https://doi.org/10.1029/JB091iB03p03664
Faure M, Lepvrier C, Nguyen VV, Vu TV, Lin W, Chen Z (2014) The South China block-Indochina collision: where, when, and how? J Asian Earth Sci 79:260–274. https://doi.org/10.1016/j.jseaes.2013.09.022
Fick SE, Hijmans RJ (2017) WorldClim 2: new 1km spatial resolution climate surfaces for global land areas. Int J Climatol 37(12):4302–4315. https://doi.org/10.1002/joc.5086
Geist EL, Yoshioka S (2004) Effect of structural heterogeneity and slip distribution on coseismic vertical displacement from rupture on the Seattle Fault. US Geological Survey, Reston
Godard V, Lavé J, Carcaillet J, Cattin R, Bourlès D, Zhu J (2010) Spatial distribution of denudation in Eastern Tibet and regressive erosion of plateau margins. Tectonophysics 491:253–274. https://doi.org/10.1016/j.tecto.2009.10.026
Ha VL, Huang HH, Huang BS, Nguyen LM, Nguyen VD, Ha TG, Le QK, Dinh QV, Le TS, Nguyen TH, Nguyen CN, Smith KK, Pham TT (2024) Geotectonic architecture beneath Northern Vietnam revealed by local earthquake tomography combining seismic data from multiple networks. Tectonophysics 884:230402. https://doi.org/10.1016/j.tecto.2024.230402
Hu X, Garzanti E, Wang J, Huang W, An W, Webb A (2016) The timing of India-Asia collision onset – facts, theories, controversies. Earth-Sci Rev 160:264–299. https://doi.org/10.1016/j.earscirev.2016.07.014
Jolivet L, Beyssac O, Goffé B, Avigad D, Lepvrier C, Maluski H, Thang TT (2001) Oligo-Miocene midcrustal subhorizontal shear zone in Indochina. Tectonics 20:46–57. https://doi.org/10.1029/2000TC900021
Joshi M, Thakur VC, Suresh N, Sundriyal YP (2022) Climate-tectonic imprints on the late Quaternary Ravi River Valley terraces of the Chamba region in the NW Himalaya. J Asian Earth Sci 223:104990. https://doi.org/10.1016/j.jseaes.2021.104990
Kirby E, Ouimet W (2011) Tectonic geomorphology along the eastern margin of Tibet: insights into the pattern and processes of active deformation adjacent to the Sichuan Basin. Geol Soc Spec Publ 353:165–188. https://doi.org/10.1144/SP353.9
Kirby E, Whipple KX (2012) Expression of active tectonics in erosional landscapes. J Struct Geol 44:54–75. https://doi.org/10.1016/J.JSG.2012.07.009
Kirby E, Johnson C, Furlong K, Heimsath A (2007) Transient channel incision along Bolinas Ridge, California: Evidence for differential rock uplift adjacent to the San Andreas fault. J Geophys Res 112:F03S07. https://doi.org/10.1029/2006JF000559
Lai K-Y, Chen Y-G, Lâm DĐ (2012) Pliocene-to-present morphotectonics of the Dien Bien Phu fault in northwest Vietnam. Geomorphology 173–174:52–68. https://doi.org/10.1016/j.geomorph.2012.05.026
Lavé J, Avouac JP (2001) Fluvial incision and tectonic uplift across the Himalayas of central Nepal. J Geophys Res Solid Earth 106:26561–26591. https://doi.org/10.1029/2001jb000359
Lee T-Y, Lawver LA (1995) Cenozoic plate reconstruction of Southeast Asia. Tectonophysics 251:85–138. https://doi.org/10.1016/0040-1951(95)00023-2
Leloup PH, Arnaud N, Lacassin R, Kienast JR, Harrison TM, Trong TTP, Replumaz A, Tapponnier P (2001) New constraints on the structure, thermochronology, and timing of the Ailao Shan-Red River shear zone, SE Asia. J Geophys Res Solid Earth 106:6683–6732. https://doi.org/10.1029/2000JB900322
Lepvrier C, Maluski H, Van Tich V, Leyreloup A, Thi PT, Van Vuong N (2004) The early Triassic Indosinian orogeny in Vietnam (Truong Son Belt and Kontum Massif); implications for the geodynamic evolution of Indochina. Tectonophysics 393:87–118
Li Z, Wang Y, Gan W, Fang L, Zhou R, Seagren EG, Zhang H, Liang S, Zhuang W, Yang F (2020) Diffuse deformation in the SE Tibetan Plateau: new insights from geodetic observations. J Geophys Res Solid Earth 125:1–18. https://doi.org/10.1029/2020JB019383
Lin T-H, Lo C-H, Chung S-L, Wang P-L, Yeh M-W, Lee T-Y, Lan C-Y, Vuong NV, Anh TT (2009) Jurassic dextral movement along the Dien Bien Phu Fault, NW Vietnam: constraints from ^{40} Ar/ ^{39} Ar geochronology. J Geol 117:192–199. https://doi.org/10.1086/595965
Liu M (2003) Extensional collapse of the Tibetan Plateau: results of three-dimensional finite element modeling. J Geophys Res 108:1–15. https://doi.org/10.1029/2002jb002248
Liu F, Yao X, Li L (2021) Applicability of geomorphic index for the potential slope instability in the three river region, eastern tibetan plateau. Sensors 21. https://doi.org/10.3390/s21196505
Lu NT, Rodkin MV, Phuong TV, Hang PTT, Quang N, Hoan VT (2016) Algorithm and program for earthquake prediction based on the geological, geophysical, geomorphological and seismic data. Vietnam J Earth Sci 38:231–241
Molnar P, Tapponnier P (1975) Cenozoic tectonics of Asia: effects of a continental collision: features of recent continental tectonics in Asia can be interpreted as results of the India-Eurasia collision. Science 189:419–426. https://doi.org/10.1126/science.189.4201.419
Molnar P, England P, Martinod J (1993) Mantle dynamics, uplift of the Tibetan Plateau, and the Indian monsoon. Rev Geophys 31:357–396. https://doi.org/10.1029/93RG02030
Nguyen V P (2006) Characteristics of bed sediments in the Da River: Grain composition, size distribution, and impact on flow (Doctoral dissertation, Hanoi University of Sciences, Vietnam). [In Vietnamese]
Ott RF, Pérez-Consuegra N, Scherler D, Mora A, Huppert KL, Braun J, Hoke GD, Sandoval Ruiz JR (2023) Erosion rate maps highlight spatio-temporal patterns of uplift and quantify sediment export of the Northern Andes. Earth Planet Sci Lett 621:118354. https://doi.org/10.1016/j.epsl.2023.118354
Pan Y, Shen WB (2017) Contemporary crustal movement of southeastern Tibet: Constraints from dense GPS measurements. Sci Rep 7:1–7. https://doi.org/10.1038/srep45348
Qiu J, Ji L, Zhu L, Li Y, Liu C, Zhao Q (2024) Coseismic deformation and seismogenic structure of the 2024 Hualien Earthquake measured by InSAR and GNSS. Earthq Res Adv 5:100328. https://doi.org/10.1016/j.eqrea.2024.100328
Rai SS, Priestley K, Gaur VK, Mitra S, Singh MP, Searle M (2006) Configuration of the Indian Moho beneath the NW Himalaya and Ladakh. Geophys Res Lett 33:3–7. https://doi.org/10.1029/2006GL026076
Roger F, Jolivet M, Maluski H, Respaut JP, Münch P, Paquette JL, Vu Van T, Nguyen Van V (2014) Emplacement and cooling of the Dien Bien Phu granitic complex: implications for the tectonic evolution of the Dien Bien Phu Fault (Truong Son Belt, NW Vietnam). Gondwana Res 26:785–801. https://doi.org/10.1016/j.gr.2013.07.018
Royden LH, Burchfiel BC, King RW, Wang E, Chen Z, Shen F, Liu Y (1997) Surface deformation and lower crustal flow in eastern Tibet. Science 276:788–790. https://doi.org/10.1126/science.276.5313.788
Royden LH, Burchfiel BC, Hilst RD (2008) The geological evolution of the Tibetan Plateau. Science 321:1054–1058
Schärer U, Tapponnier P, Lacassin R, Leloup PH, Dalai Z, Shaocheng Ji (1990) Intraplate tectonics in Asia: a precise age for large-scale Miocene movement along the Ailao Shan-Red River shear zone. China Earth Planet Sci Lett 97:65–77. https://doi.org/10.1016/0012-821X(90)90099-J
Schmidt-Thomé P, Nguyen TH, Pham TL, Jarva J, Nuottimäki K (2014) Climate change adaptation measures in Vietnam: Development and Implementation. Springer, Berlin
Schoenbohm LM, Burchfiel BC, Chen L, Yin J (2006) Miocene to present activity along the Red River fault, China, in the context of continental extrusion, upper-crustal rotation, and lower-crustal flow. Bull Geol Soc Am 118:672–688. https://doi.org/10.1130/B25816.1
Searle MP (2006) Role of the Red River Shear zone, Yunnan and Vietnam, in the continental extrusion of SE Asia. J Geol Soc London 163:1025–1036. https://doi.org/10.1144/0016-76492005-144
Searle MP, Yeh M-W, Lin T-H, Chung S-L (2010) Structural constraints on the timing of left-lateral shear along the Red River shear zone in the

Ailao Shan and Diancang Shan Ranges, Yunnan, SW China. Geosphere 6:316–338. https://doi.org/10.1130/GES00580.1
Shen Z-K, Lü J, Wang M, Bürgmann R (2005) Contemporary crustal deformation around the southeast borderland of the Tibetan Plateau. J Geophys Res Solid Earth. https://doi.org/10.1029/2004JB003421
Tan XB, Lee YH, Xu XW, Cook KL (2017) Cenozoic exhumation of the Danba antiform, eastern Tibet: evidence from low-temperature thermochronology. Lithosphere 9:534–544. https://doi.org/10.1130/L613.1
Tapponnier P, Peltzer G, Le Dain AY, Armijo R, Cobbold P (1982) Propagating extrusion tectonics in Asia: new insights from simple experiments with plasticine. Geology 10:611–616. https://doi.org/10.1130/0091-7613(1982)10%3c611:PETIAN%3e2.0.CO;2
Tapponnier P, Peltzer G, Armijo R (1986) On the mechanics of the collision between India and Asia. Geol Soc 19:113–157. https://doi.org/10.1144/GSL.SP.1986.019.01.07
Tapponnier P, Lacassin R, Leloup PH, Schärer U, Dalai Z, Haiwei W, Xiaohan L, Shaocheng J, Lianshang Z, Jiayou Z (1990a) The Ailao Shan/Red River metamorphic belt: tertiary left-lateral shear between Indochina and South China. Nature 343:431–437. https://doi.org/10.1038/343431a0
Tapponnier P, Lacassin R, Leloup PH, Schärer U, Dalai Z, Haiwei W, Xiaohan L, Shaocheng J, Lianshang Z, Jiayou Z (1990b) The Ailao Shan/Red River metamorphic belt: tertiary left-lateral shear between Indochina and South China. Nature 343:431–437. https://doi.org/10.1038/343431a0
Trinh T, Liem V, Huong V, Vinh Q, Thom V, Thao T, Tan T, Hoang N (2012) Late Quaternary tectonics and seismotectonics along the Red River fault zone, North Vietnam. Earth-Science Rev 114:224–235. https://doi.org/10.1016/j.earscirev.2012.06.008
Vinh VD, Ouillon S, Thanh TD, Chu LV (2014) Impact of the Hoa Binh dam (Vietnam) on water and sediment budgets in the Red River basin and delta. Hydrol Earth Syst Sci 18:3987–4005. https://doi.org/10.5194/hess-18-3987-2014
Viola G, Anczkiewicz R (2008) Exhumation history of the Red River shear zone in northern Vietnam: new insights from zircon and apatite fission-track analysis. J Asian Earth Sci 33:78–90. https://doi.org/10.1016/j.jseaes.2007.08.006
Wang L, Barbot S (2023) Three-dimensional kinematics of the India-Eurasia collision. Commun Earth Environ. https://doi.org/10.1038/s43247-023-00815-4
Wang CY, Zhu L, Lou H, Huang BS, Yao Z, Luo X (2010a) Crustal thicknesses and Poisson's ratios in the eastern Tibetan Plateau and their tectonic implications. J Geophys Res Solid Earth. https://doi.org/10.1029/2010JB007527
Wang Q, Wyman DA, Li ZX, Sun W, Chung SL, Vasconcelos PM, Zhang Q, Dong H, Yu Y, Pearson N, Qiu H, Zhu T, Feng X (2010b) Eocene north-south trending dikes in central Tibet: new constraints on the timing of east-west extension with implications for early plateau uplift? Earth Planet Sci Lett 298:205–216. https://doi.org/10.1016/j.epsl.2010.07.046
Whipple KX (2004) Bedrock rivers and the geomorphology of active orogens. Annu Rev Earth Planet Sci 32:151–185. https://doi.org/10.1146/annurev.earth.32.101802. 120356.
Whipple KX, Gasparini NM (2014) Tectonic control of topography, rainfall patterns, and erosion during rapid post-12 Ma uplift of the Bolivian Andes. Lithosphere 6:251–268. https://doi.org/10.1130/L325.1
Wittlinger G, Vergne J, Tapponnier P, Farra V, Poupinet G, Jiang M, Su H, Herquel G, Paul A (2004) Teleseismic imaging of subducting lithosphere and Moho offsets beneath western Tibet. Earth Planet Sci Lett 221:117–130. https://doi.org/10.1016/S0012-821X(03)00723-4
Wobus C, Whipple KX, Kirby E, Snyder N, Johnson J, Spyropolou K, Crosby B, Sheehan D (2006). Tectonics from topography: Procedures, promise, and pitfalls, In: Special Paper 398: Tectonics, Climate, and Landscape Evolution. Geological Society of America, pp. 55–74. https://doi.org/10.1130/2006.2398(04)
Wu X, Hu J, Chen L, Liu L, Liu L (2023) Paleogene India-Eurasia collision constrained by observed plate rotation. Nat Commun 14:1–10. https://doi.org/10.1038/s41467-023-42920-0
Yang J, Kaus BJP, Li Y, Leloup PH, Popov AA, Lu G, Wang K, Zhao L (2020) Lower crustal rheology controls the development of large offset strike-slip faults during the Himalayan-Tibetan orogeny. Geophys Res Lett. https://doi.org/10.1029/2020GL089435
Ye Y, Tan X, Liu Y, Zhou C, Shi F, Lee YH, Murphy MA (2022) The impact of erosion on fault segmentation in thrust belts: insights from thermochronology and fluvial shear stress analysis (southern Longmen Shan, eastern Tibet). Geomorphology 397:108020. https://doi.org/10.1016/j.geomorph.2021.108020
Yeh M-W, Lee T-Y, Lo C-H, Chung S-L, Lan C-Y, Anh TT (2008) Structural evolution of the Day Nui Con Voi metamorphic complex: implications on the development of the Red River Shear Zone, Northern Vietnam. J Struct Geol 30:1540–1553. https://doi.org/10.1016/J.JSG.2008.08.007
Yu L, Dong Y, Zhou W, Zhang D, Wang D, Yu H, Ren Y, Li J (2022) Evaluation of the rock uplift pattern in the Central Yunnan Subblock, SE Tibetan Plateau: based on the bedrock channel profile. Front Earth Sci 10:1–15. https://doi.org/10.3389/feart.2022.821367
Zhang P-Z, Shen Z, Wang M, Gan W, Bürgmann R, Molnar P, Wang Q, Niu Z, Sun J, Wu J, Hanrong S, Xinzhao Y (2004) Continuous deformation of the Tibetan Plateau from global positioning system data. Geology 32:809–812. https://doi.org/10.1130/G20554.1
Zuchiewicz W, Cuong NQ, Bluszcz A, Michalik M (2004) Quaternary sediments in the Dien Bien Phu fault zone, NW Vietnam: a record of young tectonic processes in the light of OSL-SAR dating results. Geomorphology 60:269–302. https://doi.org/10.1016/J.GEOMORPH.2003.08.004

Publisher's Note